Impacts of Sea-Level Rise on Subsurface Water Environment in the Lower Seyhan River Basin

—Calibrated and Projected Results—

Katsuyuki FUJINAWA[1] and Takeshi ARIMA[2]
[1,2]*Geo-environmental engineering, Faculty of engineering, Shinshu University*
550 Wakasato, Nagano, Nagano 380-8533, JAPAN
e-mail:[1]fujinawa@shinshu-u.ac.jp, [2]t04a302@amail.shinshu-u.ac.jp

1. Introduction

According to IPCC, global warming is expected to cause sea-level rise, which affects such subsurface water environment as salt water intrusion, groundwater flow, salt transport, etc. The objective of this study is to develop a mathematical model for analyzing the subsurface water environment of the Lower Seyhan River Basin (LSRB), Turkey, and to project the impacts of seal-level rise.

Fig.1 shows a procedure for projecting the impacts of sea-level rise by using numerical simulations. The core of the projection is a newly developed 2D saltwater intrusion model, SIFEC, which is based on coupling of the Galerkin-finite element method for saturated-unsaturated, density-dependent flow and the method of characteristics for mass transport. High performance of SIFEC in terms of accuracy has already been proved (Fujinawa et al, 2005) and its applicability was also shown by an example applied to a problem of salt-water intrusion into coastal aquifers in small islands (Tomigashi and Fujinawa, submitted for publication).

Provided with future changes in precipitation, evapotranspiration, irrigation practices, etc, SIFEC can be applied to assess impacts of climate change on availability of groundwater resources, groundwater salinity, water logging, and salt accumulation on land surface. A physical model to describe groundwater flow and salt transport in subsurface environment was first constructed by taking into account geologic and geographic properties of LSRB.

The model was then calibrated by using such observed or estimated hydrogeologic parameters as hydraulic conductivities, strativities, effective porosities, soil-moisture characteristics, longitudinal and transverse dispersivities, together with salinity distribution in aquifers, rate and distribution of recharge, and groundwater withdrawal so that the calculated and the observed groundwater table coincide.

The model was finally run under several scenarios with respect to sea-level rise. Other runs for scenarios with respect to recharge rates and groundwater withdraw rates will be followed soon. The projected results of the water environment in LSRB are discussed in this report.

2. Preparation of Input Data

The 2D vertical model used covers a profile of 50 km long and 300 m deep, while its transect was chosen so that it passes the city of Adana and the Akyatan lagoon, and is perpendicular to observed equi-potential lines. Its geologic structure has already been reported in the former publication of ICCAP. A mathematical model requires a set of physical parameters such as hydraulic conductivity, effective porosity, strativity, soil-water characteristic properties, and longitudinal and transverse dispersivity. The geologic units of LSRB are consisted of four types of formations; aquifer, sand dune, clayey layer, and basal layer. The hydrogeologic properties of these layers are given in Table 1.

Boundary conditions are set by using observed groundwater table height, salinity of groundwater, sea and/or lagoon

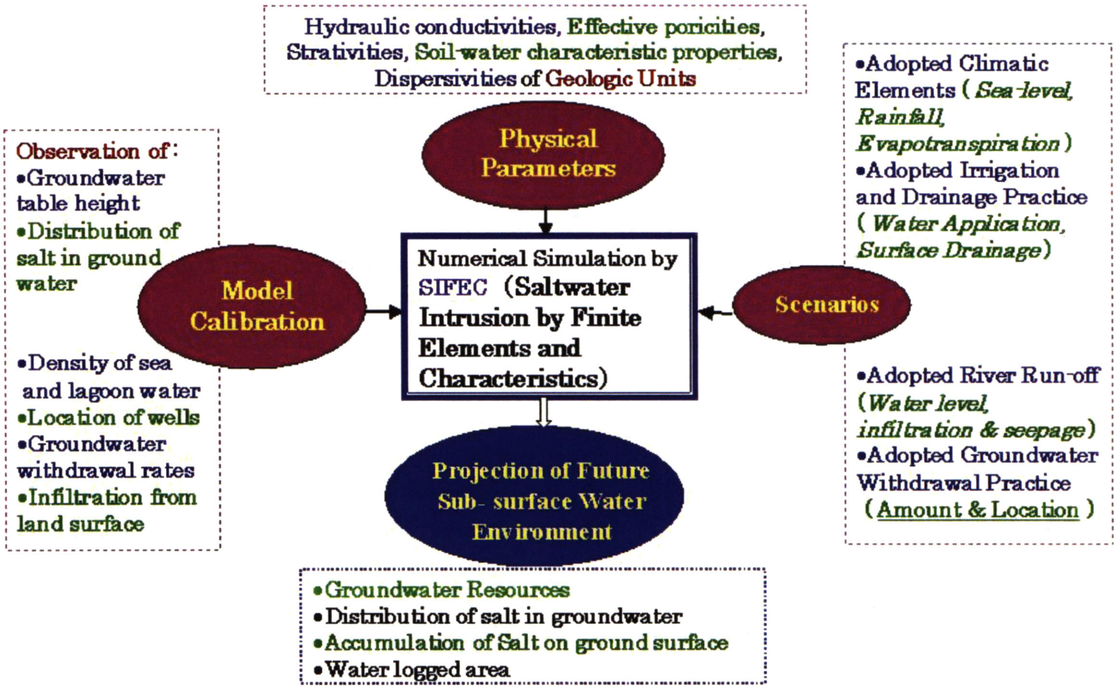

Fig.1 Procedure for Projecting the Impacts of Sea-Level Rise

Hydraulic Conductivity (m/day)	**Aquifer : 86.00** **Sand Dune : 34.50** **Clayey Layer : 0.22** **Base : 0.04**
Effective Porocity	**All Layer : 0.22**
Longitudinal Dispersivity (m)	**All Layer : 30.0**
AT/AL	**1/10 (=3.0)**

Table 1 Hydrogeologic Properties of Geologic Units

Boundary Conditions for GW Flow Eq.
Fresh water on the left side=18.7(m)
Sea water on the right side =0.0(m)
Lagoon water=0.0(m)

Boundary Conditions for Mass Trans. Eq.
Fresh water on the left side= 1.002(g/cm³)
Sea water on the right side =1.030(g/cm³)
Lagoon water=1.030(g/cm³)

Table 2 Boundary conditions

water together with infiltration rate along land surface of the domain. Table 2 shows those conditions used for calibration runs.

Daily average recharge rate was determined as 1.5mm/day for irrigated area, 0.71mm/day for non-irrigated area north of the Akyatan lagoon, and 0.36mm/day for dune area by using monthly data of precipitation, irrigation, evapo-transpiration that was calculated by the Thornthwaite method.

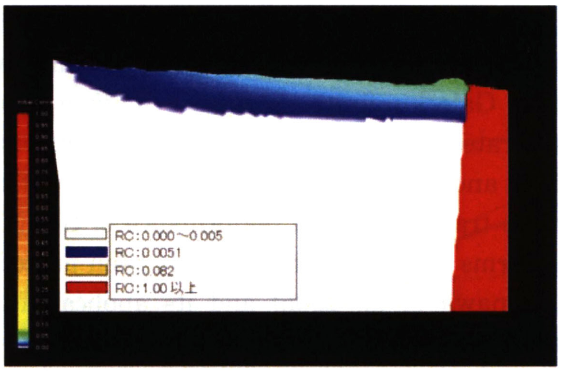

Fig.2 Initial concentration distribution of salinity relative to Mediterranean Sea

Initial distribution of salinity in shallow groundwater was determined by referring to soil and groundwater salinity data provided by DSI. It was assumed that the initial salinity of shallow groundwater gradually decreases downward upto 50 m deep from mean sea level, and the rest of the regional groundwater has a constant EC of 0.02 S/m. Furthermore, a sharp initial interface was also assumed between salt and fresh groundwater, which locates with slightly inclined straight line from vertical direction. Fig.2 shows the initial distribution of relative salinity concentration.

3. Calibrated Results

Model outputs in terms of piezometric head and salt concentration were compared with those of observed values, and calibration runs were repeated until both results coincide to a satisfactory degree. Fig.3 shows a comparison between observed and calculated groundwater table. The maximum error was 0.4 m at well no.417.

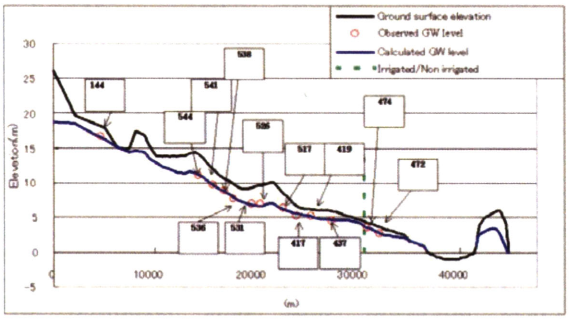

Max Error: 0.40m at well no.417

Fig.3 Comparison between Observed and Calculated Groundwater Table

Fig.4 illustrates finite elements together with locations of well screens. Groundwater withdrawal rates below the figure indicate values inversely identified so as for the discrepancy between the observed and the calculated hydraulic head to be minimized.

Salt is accumulated on land surface at the area close to the lagoon where seepage face is formed. The accumulation can be evaluated from seepage rate calculated as outward groundwater flux to the seepage face and its concentration. Calculated salt accumulation for the calibration run is restricted only to the area as far as 1,866m from the shore of the lagoon.

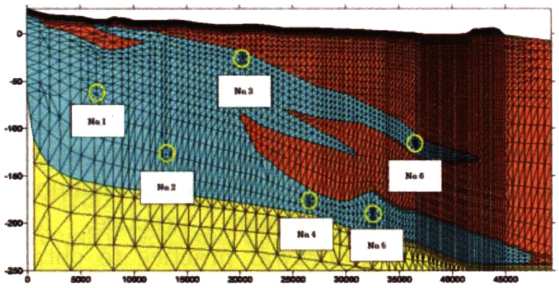

No.1=No.2=9.50(m^3/day), No.3=19.09(m^3/day), No.4=9.21(m^3/day) No.5=5.77(m^3/day), No.6=1.26(m^3/day)

Fig.4 Finite Element Mesh and Location of Well Screens

Water level of the lagoon was maintained to be the same as the Mediterranean throughout the simulation since both water is connected via a narrow stream. However, condensation of the lagoon water has been taking place due to the seepage of saline groundwater and evaporation from the water surface. Observation of the salinity distribution of the Akyatan lagoon revealed that mean EC of the deeper part is 10.0 S/m and that of the shallower part is 7.8 S/m, while that of the Mediterranean is 5.8 S/m. Concentration of the lagoon water can also be calculated using the seepage rate and the mass of salt transported by the seepage flow.

During the calibration run, concentration

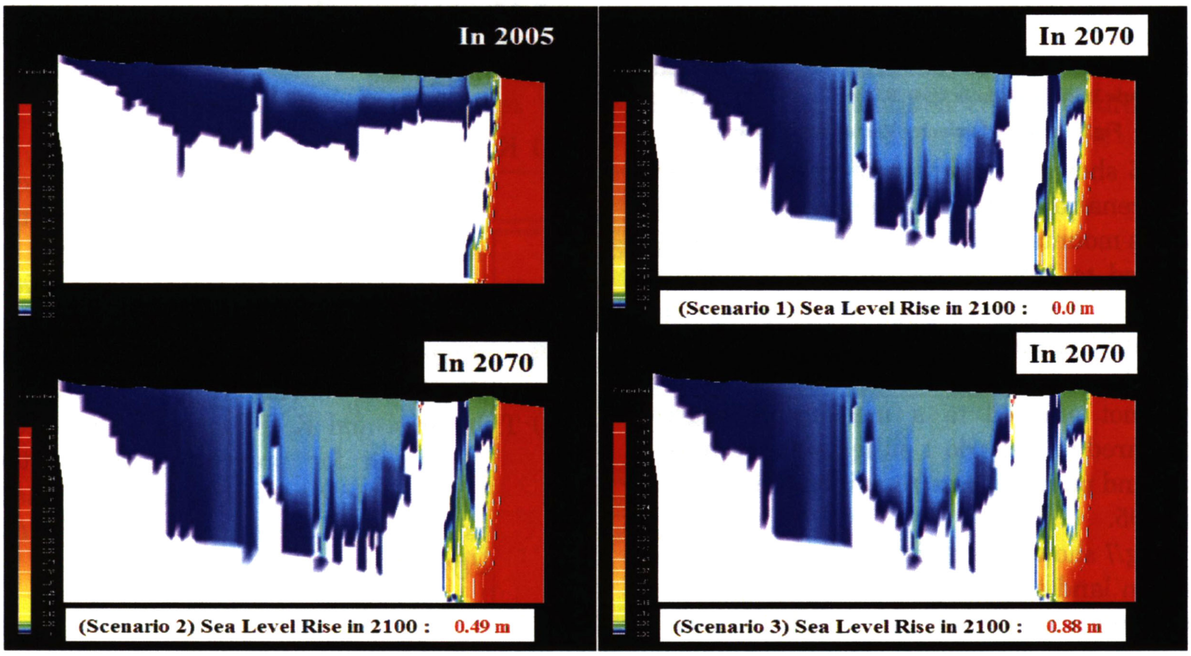

Fig.5 Projected Concentration for Three Types of Scenarios

of the lagoon water gradually increased from the initial concentration (EC=5.8 S/m), which is the same as the Mediterranean, to the current observed concentration of the Akyatan lagoon (EC=6.8 S/m).

4. Some Projected Results

Followed by the calibration process, the fixed model are then used to run for various scenarios based on climatic elements, irrigation and drainage practice, and groundwater withdrawal practice to obtain future projection of groundwater flow, salinity of groundwater, accumulation of salt on land surface, water logging, etc.

Possible factors for the scenarios can be consisted of see-level rise, recharge rate, and pumping rate. Any combination of these factors makes up scenarios.

Fig.5 shows projected concentration distributions in 2070 for three types of scenarios where only sea levels were changed. Sea level rise of as much as 0.88 m/ century does not seem to affect concentration distribution significantly.

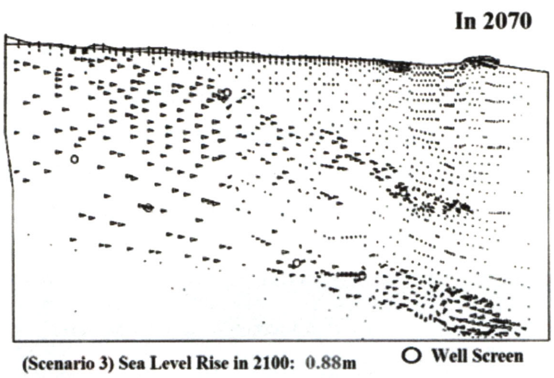

Fig.6 Projected velocity Vector for Scenario 3

Fig. 6 shows distribution of velocity vectors for scenario 3. The amount of inflow rate across mountain-side boundary for scenario 3 reduced to 1597 m^3/year/m from scenario 1 of 1632 m^3/year/m due to reduction in hydraulic gradient accompanied by sea-level rise. Groundwater table height for scenario 3 was not affected to a measurable degree compared to scenario 1 either, since recharge rate and pumping rate remained the same as in 2005.

Fig.7 shows the projected accumulation of salt on land surface for scenario 3. The salt accumulation increased drastically compared to the calibration run.

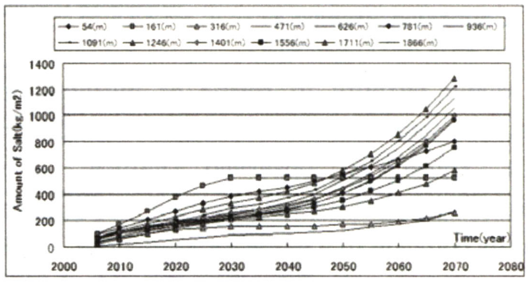

Fig.7 Accumulation of Salt on Land Surface for Scenario

Fig.8 shows the projected change in concentration of the lagoon water for scenario 3. It was assumed that the level of the Mediterranean rises 0.572 m in 2070 and its salt concentration remains unchanged throughout the projection period. Furthermore, the level of the lagoon water is also assumed to be the same as the Mediterranean, which means that the lagoon is supplied with the sea water via the stream. Fig.8 suggests that salt supplied by discharging groundwater and evaporation of water from the lagoon is not enough to increase the concentration of the lagoon water due to supply of sea water with constant salinity.

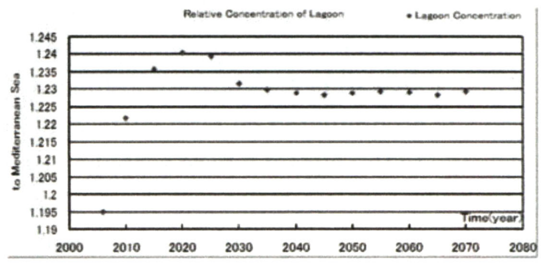

Fig.8 Projected Change in Rerative Concentration of Lagoon Wat

5. References

(1) K. Fujinawa, K. Masuoka, T. Nagano, T. Watanabe, (2004): Numerical simulation modeling for salt-water intrusion in predicting impacts of sea-level rise on areas below sea-level, *Journal of Environmental Systems and Engineering, Japan Society of Civil Engineers*, No.790/VII-35,pp.35-48.

(2) T.Tomigasi and K. Fujinawa (submitted): Measures for preventing salt water intrusion into coastal aquifers in small islands, *Journal of Groundwater Hydrology*